

HEAVY QUARK HADROPRODUCTION IN k_T -FACTORIZATION APPROACH AND THE EXPERIMENTAL DATA

Yu.M.Shabelski and A.G.Shuvaev
Petersburg Nuclear Physics Institute,
Gatchina, St.Petersburg 188350 Russia

Abstract

We compare the numerical predictions of the k_T -factorization approach (semi-hard theory) for heavy quark production in high energy nucleon-nucleon and photon-nucleon collisions with the experimental data from Tevatron-collider and HERA. Predictions for heavy quark production at Tevatron, LHC and HERA are also presented.

E-mail SHABELSK@THD.PNPI.SPB.RU

E-mail SHUVAEV@THD.PNPI.SPB.RU

1 Introduction

The investigation of heavy quark production in high energy hadron collisions is an important method for studying the quark-gluon structure of hadrons. The description of hard interactions in hadron collisions within the framework of QCD is possible only with the help of some phenomenology, which reduces the hadron-hadron interaction to the parton-parton one via the formalism of the hadron structure functions. The cross sections of hard processes in hadron-hadron interactions can be written as the convolutions of sub-process QCD matrix elements squared with the parton distributions in the colliding hadrons.

The most popular and technically simplest approach is the so-called QCD collinear approximation, or parton model (PM). In this model all particles involved are assumed to be on mass shell, carrying only longitudinal momenta, and the cross section is averaged over two transverse polarizations of the incident gluons. The virtualities q^2 of the initial partons are taken into account only through their structure functions. The cross sections of QCD subprocess are calculated usually in the next to leading order (NLO) [1, 2, 3, 4, 5] of α_S expansion. The transverse momenta of the incident partons are neglected in the QCD matrix elements. This is the direct analogy of the Weizsaecker-Williams approximation in QED.

Another possibility to incorporate the incident parton transverse momenta is referred to as k_T -factorization approach [6, 7, 8, 9, 10, 11], or the theory of semihard interactions [12, 13, 14, 15, 16, 17, 18, 19, 20]. Here the Feynman diagrams are calculated with account of the virtualities and possible polarizations of the incident partons. In the small x domain there are no grounds to neglect the transverse momenta of the gluons, q_{1T} and q_{2T} , in comparison with the quark mass and transverse momenta, p_{iT} . Moreover, at the very high energies and p_{iT} the main contribution to the cross sections comes from the region $q_{1T} \sim p_{1T}$ or $q_{2T} \sim p_{1T}$, see [21, 22, 23] for details. The QCD matrix elements of the sub-processes are rather complicated in such an approach. We have calculated them in the LO. On the other hand, the multiple emission of soft gluons is effectively included here. That is why it is the question which approach is more constructive.

The k_T -factorization approach is based on so-called unintegrated parton distributions which, at the moment, are known with insufficient accuracy. Here we find them with the help of the realistic gluon distribution GRV94 [24] which is compatible with the most recent data, see discussion in Ref. [25].

In Sect. 2 we present very shortly the formalism of the k_T -factorization approach. The comparison of our numerical results with some experimental data on beauty production at Tevatron-collider together with the predictions including LHC energy are discussed in Sect. 3. Predictions of the k_T -factorization approach for heavy quark photoproduction for HERA are given in Sect. 4.

2 Heavy quark production in the k_T -factorization approach

The main contribution to the cross section of heavy quark production at small x is known to come from $gg \rightarrow Q\bar{Q}$ subprocess (and $\gamma g \rightarrow Q\bar{Q}$ in the case of photoproduction). The transverse momenta of the incident gluons in the small- x region result in the k_T -factorization approach from $\alpha_S \ln k_T^2$ gluon diffusion. This is described by the so-called unintegrating gluon distribution which can be written in the form [22, 26, 27]

$$f_g(x, q_T, \mu) = \sum_{a'} \left[\frac{\alpha_s}{2\pi} \int_x^\Delta P_{ga'}(z) a' \left(\frac{x}{z}, q_T^2 \right) dz \right] T_g(q_T, \mu), \quad (1)$$

where the survival probability T_g that gluon g with the transverse momentum q_T remains untouched in the evolution up to the factorization scale μ is

$$T_g(q_T, \mu) = \exp \left[- \int_{q_T^2}^{\mu^2} \frac{\alpha_s(p_T)}{2\pi} \frac{dp_T^2}{p_T^2} \sum_{a'} \int_0^\Delta P_{a'g}(z') dz' \right]. \quad (2)$$

Here $a'(x, q_T^2)$ denotes $xg(x, q_T^2)$ or $xq(x, q_T^2)$, and $P_{ga'}(z)$ are the splitting functions.

We have to emphasize that $f_g(x, q_T, \mu)$ is just the quantity which enters into the Feynman diagrams. The distributions $f_g(x, q_T, \mu)$ involve two hard scales¹: q_T and the scale μ of the probe. The scale μ plays a dual role. On the one hand it acts as the factorization scale, while on the other hand it controls the angular ordering of the partons emitted in the evolution [28, 29, 30]. The factorization scale μ separates the partons associated with the emission off both the beam and target protons (in pp collisions) and off the hard subprocess. For example, it separates emissions off the beam (with polar angle $\theta < 90^\circ$ in c.s.m.) from those off the target (with $\theta > 90^\circ$ in c.s.m.), and from the intermediate partons from the hard subprocess. This separation was proved in [28, 29, 30] and originates from the destructive interference of the different emission amplitudes (Feynman diagrams) in the angular boundary regions.

If the longitudinal momentum fraction is fixed by the hard subprocess, then the limits of the angles can be expressed in terms of the factorization scale μ which corresponds to the upper limit of the allowed value of the s -channel parton k_T .

The expression (1) with the survival probability (2) provides the positivity of the unintegrated probability $f_g(x, q_T, \mu)$ in the whole interval $0 < x < 1$.

Here we deal with the matrix element accounting for the gluon virtualities and polarizations. Since it is much more complicated than in the PM we consider only the LO of the subprocess $gg \rightarrow Q\bar{Q}$ which gives the main contribution to the heavy quark production cross section at small x , see the diagrams a, b and c in Fig. 1. The lower and upper ladder blobs present the unintegrating gluon distributions $f_g(y, q_{1T}, \mu)$ and $f_g(x, q_{2T}, \mu)$.

¹This property is hidden in the conventional parton distributions as q_T is integrated up to the scale μ .

The differential cross section of heavy quark hadroproduction has the following form:²

$$\begin{aligned} \frac{d\sigma_{pp}}{dy_1^* dy_2^* d^2p_{1T} d^2p_{2T}} &= \frac{1}{8\pi^2} \frac{1}{(s)^2} \int d^2q_{1T} d^2q_{2T} \delta(q_{1T} + q_{2T} - p_{1T} - p_{2T}) \\ &\times \frac{\alpha_s(q_1^2)}{q_1^2} \frac{\alpha_s(q_2^2)}{q_2^2} f_g(y, q_{1T}, \mu) f_g(x, q_{2T}, \mu) |M_{QQ}|^2. \end{aligned} \quad (3)$$

Here $s = 2p_A p_B$, $q_{1,2T}$ are the gluon transverse momenta and $y_{1,2}^*$ are the heavy quark rapidities in the hadron-hadron c.m.s. frame,

$$\begin{aligned} x_1 &= \frac{m_{1T}}{\sqrt{s}} e^{-y_1^*}, & x_2 &= \frac{m_{2T}}{\sqrt{s}} e^{-y_2^*}, & x &= x_1 + x_2 \\ y_1 &= \frac{m_{1T}}{\sqrt{s}} e^{y_1^*}, & y_2 &= \frac{m_{2T}}{\sqrt{s}} e^{y_2^*}, & y &= y_1 + y_2 \\ m_{1,2T}^2 &= m_Q^2 + p_{1,2T}^2. \end{aligned} \quad (4)$$

$|M_{QQ}|^2$ is the square of the matrix element for the heavy quark pair hadroproduction. It is calculated in the Born approximation of QCD without standard simplifications of the parton model. Contrary to what is mentioned in [19], the transformation Jacobian from x, y to y_1^*, y_2^* is included in our matrix element.

We take

$$m_c = 1.4 \text{ GeV}, \quad m_b = 4.6 \text{ GeV}, \quad (5)$$

for the values of short-distance perturbative quark masses [32, 33].

3 Beauty production at Tevatron-collider

Eq. (3) enables us to calculate straightforwardly all one-particle distributions as well as correlations between two produced heavy quarks using, say, the VEGAS code [34].

However there exists a principle problem coming from the infrared region. Since the functions $f_g(y, q_{1T}, \mu)$ and $f_g(x, q_{2T}, \mu)$ are unknown at small values of q_2^2 and q_1^2 , i.e. in nonperturbative domain we calculate separately the contributions from $q_1^2 < Q_0^2$, $q_2^2 < Q_0^2$, $q_1^2 > Q_0^2$ and $q_2^2 > Q_0^2$ [21, 22, 23].

The first contribution ($q_1^2 < Q_0^2$, $q_2^2 < Q_0^2$) with the matrix element averaged over directions of the two-dimensional vectors q_{1T} and q_{2T} is exactly the same as the conventional LO parton model expression. It is multiplied by the 'survival' probability $T^2(Q_0^2, \mu^2)$. (We assume $Q_0^2 = 1 \text{ GeV}^2$ in the following numerical calculations.) In this contribution the sum of the produced heavy quark transverse momenta is taken to be exactly zero.

The next three contributions (from the domains where one, or both $q_i^2 > Q_0^2$) contain the corrections to the parton model matrix element due to gluon polarizations, virtualities and transverse momenta. Their relative contribution strongly depends on the initial energy. If it is not high enough, the first term dominates, and all results are similar

²We put the argument of α_s to be equal to gluon virtuality, which is very close to the BLM scheme[31]; (see also [15]).

to the conventional LO parton model predictions [22]. In the case of very high energy the opposite situation takes place, the first term can be considered as a small correction and our results differ from the conventional ones. So the highest energies are needed to observe (and to study) the k_T -factorization effects.

In the numerical calculations some uncertainties come from the value of cut-off Δ in Eqs. (1), (2). In particular, in [22] we used

$$\Delta = 1 - q_T/\mu . \quad (6)$$

The angular ordering [28, 29, 30] implies that the cut-off

$$\Delta = \frac{\mu}{\mu + q_T} . \quad (7)$$

In this case one gets the non-zero values of $f_a(x, q_T, \mu)$ even at the large $q_T > \mu$. This is especially important at the high energies where the essential values of x and z in Eqs. (1), (2) are very small.

From the formal point of view the difference between (6) and (7) is beyond the DGLAP LO accuracy. With the same accuracy we can suggest

$$\Delta = \frac{\mu}{\sqrt{\mu^2 + q_T^2}} , \quad (8)$$

or something like that.

Another source of uncertainties comes from the fact that the unintegrated gluon distributions are not known with the needed accuracy (from the evolution equation and the experimental data).

Let us compare the results of our numerical calculations with the data on beauty production at Tevatron-collider. In Fig. 2a we present the data [35] on $b\bar{b}$ pair production with $p_T > p_{min}$ identified by their muon decays, as the function of p_{min} at $\sqrt{s} = 1.8$ TeV. The curves of different type show the calculated results with different cut-off Δ in (1) and (2), whereas the upper and lower curves of the same type are obtained with different QCD scales, $\mu^2 = \hat{s}$ and $\mu^2 = \hat{s}/4$, where \hat{s} is the invariant energy of the produced heavy quark pair, $\hat{s} = xys$.

One can see that the scale dependence is negligible here. The dependence on the cut-off Δ is more important. The expressions (6) (dash-dotted curves) and (7) (dashed curves) give too small cross section, whereas the cut-off (8) (dotted curves) overestimates the data. We obtain the best agreement with the experiment (solid curves), assuming the cut-off smaller than (8) and larger than (7), namely

$$\Delta = \frac{\mu}{\sqrt{\mu^2 + q_T^2 + \mu q_T}} . \quad (9)$$

The same results for inclusive b -quark production at large p_T extracted from muon tagged jets [36] are presented in Fig. 2b. Here again the data are in reasonable agreement with our calculations using Eq. (9).

The rapidity distributions of the produced beauty [37] are shown in Fig. 3a, b. They decrease more steeper than our predictions, but the numerical difference is not large.

The correlation between the produced heavy quark and antiquark [11, 38] which are more sensitive to the dynamics of the production mechanism are presented in Fig. 4. Here the transverse momentum of one beauty quark, p_{1T} , is taken more than some value (6.5 GeV in Fig. 4a and 8.75 GeV in Fig. 4b), and cross sections of second quark production with $p_{2T} > p_{min}$ are presented as the functions of p_{min} . Again, these data can be described using the cut-off (9).

There are the correlations which are more sensitive to the QCD scale value μ in comparison with the cut-off value. Some examples are presented in Fig. 5, where the distributions over the pair transverse momenta are plotted with the condition that one heavy quark has fixed (and large) transverse momentum. In all cases the shapes of the curves calculated with $\mu^2 = \hat{s}$ and $\mu^2 = \hat{s}/4$ are qualitatively different.

The results for the total cross sections of heavy quark production at FNAL and LHC are presented in the Table. These cross sections are essentially larger in comparison with the conventional NLO QCD predictions, see, e.g. [39]. It can be important for the planning of the experiments at LHC.

The total cross sections of charm and beauty production calculated in the
 k_T -factorization approach with cut-off (9) and $\mu^2 = \hat{s}$

	all rapidities		$ y_1^* < 1, y_2^* < 1$	
\sqrt{s}	$c\bar{c}$	$b\bar{b}$	$c\bar{c}$	$b\bar{b}$
14 TeV	20.9 mb	1.16 mb	2 mb	142 μ b
1.8 TeV	3.15 mb	107 μ b	423 μ b	20 μ b

The azimuthal correlations of heavy quarks, i.e. the distribution over the opening angle ϕ between the momentum vectors of the produced quarks in the plane transverse to the beam axis, are sensitive to the details of the production mechanism. For example, the experimental data at fixed target energies are in contradiction with NLO QCD collinear approximation [40, 41]. Our predictions for $b\bar{b}$ production at 1.8 TeV and 14 TeV are presented in Fig. 6. The same predictions obtained for the large transverse momenta of both quarks, $p_{1,2T} > 6$ GeV, are also shown.

4 Heavy quark photoproduction

In the case of high energy heavy quark photoproduction we should consider (in LO QCD) two possibilities, direct production in the photon-gluon fusion, $\gamma p \rightarrow Q\bar{Q}$, Fig. 7, and the resolved production via quark-gluon structure of the photon. In the latter case the diagrams are similar to those in Fig. 1, where one proton should be replaced by photon.

The cross section of the direct interaction can be written as

$$\frac{d\sigma_{\gamma p}}{d^2p_{1T}} = \frac{\alpha_{em}e_Q^2}{\pi} \int dz d^2q_T \frac{f_g(x, q_T, \mu)}{q_T^4} \alpha_s(q^2) \times \left\{ [(1-z)^2 + z^2] \left(\frac{\vec{p}_{1T}}{D_1} + \frac{\vec{q}_T - \vec{p}_{1T}}{D_2} \right)^2 + m_Q^2 \left(\frac{1}{D_1} - \frac{1}{D_2} \right)^2 \right\}, \quad (10)$$

$$D_1 = p_{1T}^2 + m_Q^2, \quad D_2 = (\vec{q}_T - \vec{p}_{1T})^2 + m_Q^2, \quad (11)$$

where $\alpha_{em} = 1/137$ and e_Q is the electric charge of the produced heavy quark.

The resolved contribution is determined by Eq. (3), where one of the structure functions f_g describes the partons distribution in the proton and the other stands for the parton distribution in the photon.

The energy dependences of the total cross sections of $c\bar{c}$ and $b\bar{b}$ photoproduction are presented in Fig. 8. The predictions for the cross sections of charm photoproduction together with the data [42, 43] are shown in Fig. 8a. The averaged cross section value at low energies is taken from [43]. The data on beauty photoproduction citeH1 are shown in Fig. 8b. The cut-off value (9) is again in reasonable agreement with the data. The values (6) and (7) give too small cross section, as well as NLO QCD approach [44]. These results are in agreement with [45], where different assumptions were used.

We can see that the cut-off expression (9) gives a better agreement with all the presented data in comparison with the other expressions (6)-(8). The μ^2 dependence of all distributions is rather weak except of the special case similar to Fig. 5. So, as a rule, we will present below the results obtained with the cut-off (9) and $\mu^2 = \hat{s}$ only.

The one-particle p_T -distributions, $d\sigma/dp_T$, calculated in the k_T -factorization approach for HERA energy, are presented in Fig. 9. Here we give separately the sum of direct and resolved contributions, as well as the only resolved ones. The resolved contributions decrease with p_T more fast, that is connected with the finite phase space value. At very high energies the resolved contributions will decrease more slow.

The predicted rapidity distributions, $d\sigma/dy^*$, of the produced heavy quarks are shown in Fig. 10 for all events and for events with $p_T > 6$ GeV. The direct production gives the narrow peak in the photon fragmentation region. This peak moves to the central region when only quarks with high transverse momenta are registered, that is in agreement with the data [46]. The resolved photon contribution dominates in the target fragmentation and partly in the central regions.

The distributions of pair transverse momenta with the condition that one heavy quark has fixed (and large in comparison with its mass) transverse momentum are given in Fig. 11. Here again, as in Fig. 5, the shapes of the curves calculated with $\mu^2 = \hat{s}$ and $\mu^2 = \hat{s}/4$ are qualitatively different that allows one to determine the scale value.

The predictions for the azimuthal correlations in heavy quark photoproduction at HERA energy are presented in Fig. 12. Their dependences on ϕ and on the restriction of the minimal transverse momenta of the produced quarks are qualitatively similar to the case of hadroproduction shown in Fig. 6.

5 Conclusion

We have compared the k_T -factorization approach for heavy quark hadro- and photoproduction at collider energies with the existing experimental data. The agreement is reasonable when we take the cut-off (9) in Eqs. (1) and (2) while it does not practically depends on the value of QCD scale μ in these equations. We present also predictions which can be used as an additional test of our approach. Let us note that the different expressions for the cut-off Δ result mainly into normalization factor only, so our predictions from [22, 23] obtained with the cut-off (6) can be used after renormalization with the cut-off (9) too.

Another example of very successful agreement between experimental data and k_T -factorization approach can be found in Ref.[11] based on different assumptions.

We hope that future experiments will allow to distinguish between various approaches. It is necessary to note that the theoretical results concern the heavy quarks rather than experimentally observed hadron production. The hadronization leads to several important effects, however their description needs additional phenomenological assumptions, see e.g. [47, 48, 49, 50, 51].

Acknowledgements

We are grateful to M.G.Ryskin for a lot of very useful discussions and L.K.Gladilin for outlook the experimental situation at HERA. This work was supported by grants NATO PSTCLG 977275 and RFBR 01-02-17095 and by the "Vedusch. Nauch. Shcool" RFFI 00-15-96610.

Figure Captions

Fig. 1. Low order QCD diagrams for heavy quark production in pp ($p\bar{p}$) collisions via gluon-gluon fusion.

Fig. 2. The cross sections for beauty production with $|y_1| < 1$, in $p\bar{p}$ collisions at 1.8 TeV and their description by the k_T -factorization approach with unintegrated gluon distribution $f_g(x, q_T, \mu)$ given by Eq. (1). The values of Δ in Eq. (1), (2) are taken equal to $\mu/\sqrt{(q_T^2 + \mu^2)}$ (dotted curves), to $\mu/\sqrt{(q_t^2 + \mu^2 + q_t\mu)}$ (solid curves), to $\mu/(q_T + \mu)$ (dashed curves) and to $1 - q_T/\mu$ (dash-dotted curves). The upper curves in the left-hand side of Fig. 2a correspond to the scale value in Eqs. (1) and (2) $\mu^2 = \hat{s}/4$, and the lower curves to the scale value $\mu^2 = \hat{s}$. In the case of Fig. 2b upper curves correspond to $\mu^2 = \hat{s}$ and lower ones to $\mu^2 = \hat{s}/4$.

Fig. 3 The rapidity dependences of beauty production detected by decay muons with $p_T^\mu > 5$ GeV (a) and $p^\mu > 8$ GeV (b) at 1.8 TeV. The curve types are the same as in Fig. 2.

Fig. 4. Semi differential $b\bar{b}$ cross sections at $|y_1| < 1$, $|y_2| < 1$, $p_{1Tmin} = 6.5$ GeV (a) and 8.75 GeV (b) and their description by the k_T -factorization approach with unintegrated gluon distribution $f_g(x, q_T, \mu)$ given by Eq. (1). The curve types are the same as in Fig. 2.

Fig. 5. The distributions of the total transverse momentum p_{pair} for $b\bar{b}$ production in $p\bar{p}$ collisions at $\sqrt{s} = 1.8$ TeV (a) and 14 TeV (b) and with the transverse momentum of one heavy quark equal to 20 GeV, calculated with the unintegrated gluon distribution $f_g(x, q_T, \mu)$ given by Eq. (1). The curve types are the same as in Fig. 2. The curves 1 are calculated with scale μ^2 equal to \hat{s} , and the curves 2 with the scale $\mu^2 = \hat{s}/4$.

Fig. 6. The azimuthal angle distributions of b quarks with $|y_1^*| < 1$ and $|y_2^*| < 1$ produced in pp ($p\bar{p}$) collisions at 1.8 TeV (solid and dotted curves) and at 14 TeV (dashed and dash-dotted curves) for all p_T of the produced quarks (solid and dashed curves) and for both $p_{1T}, p_{2T} > 6$ GeV (dotted and dash-dotted curves).

Fig. 7. Low order QCD diagrams for heavy quark production in direct γp interactions via photon-gluon fusion.

Fig. 8. Total cross section of heavy quark photoproduction. The Δ values in Eq. (1), (2) are taken equal to $\mu/\sqrt{(q_T^2 + \mu^2)}$ (dotted curves), to $\mu/\sqrt{(q_t^2 + \mu^2 + q_t\mu)}$ (solid curves) and to $\mu/(q_T + \mu)$ (dashed curves). The curves 1 are calculated with scale μ^2 equal to \hat{s} , and the curves 2 with scale $\mu^2 = \hat{s}/4$.

Fig. 9. The calculated p_T -distributions of charm and beauty photoproduction at $W = 200$ GeV (solid and dashed curves) with Δ in Eq. (1), (2) equal to $\mu/\sqrt{(q_T^2 + \mu^2 + q_T\mu)}$ and scale $\mu^2 = \hat{s}$. The resolved photon contributions are shown by dotted and dash-dotted curves, respectively.

Fig. 10. The calculated rapidity distributions of charm (a) and beauty (b) photoproduction at $W = 200$ GeV for all p_T (solid curve) and $p_T > 6$ GeV (dashed curve) with Δ in Eq. (1), (2) equal to $\mu/\sqrt{(q_T^2 + \mu^2 + q_T\mu)}$ and scale $\mu^2 = \hat{s}$. The resolved photon

contributions for the presented two cases are shown by dotted and dash-dotted curves, respectively.

Fig. 11. The distributions of the total transverse momentum p_{pair} for $c\bar{c}$ and $b\bar{b}$ produced in γp collisions at $W = 200$ GeV, and with the transverse momentum of a one heavy quark equal to 10 GeV, calculated with the unintegrated gluon distribution $f_g(x, q_T, \mu)$ given by Eq. (1). The values of Δ in Eq. (1), (2) are taken equal to $\mu/\sqrt{(q_T^2 + \mu^2 + q_T\mu)}$. The curves 1 are calculated with scale μ^2 equal to \hat{s} , and the curves 2 with the scale $\mu^2 = \hat{s}/4$.

Fig. 12. The azimuthal angle distributions of c and b quarks with all rapidities produced in γp collisions at 200 GeV for all p_T of produced quarks (solid and dashed curves, respectively), for $p_{1T}, p_{2T} > 2$ GeV for charm production (dotted curve) and for $p_{1T}, p_{2T} > 5$ GeV for beauty production (dash-dotted curves).

References

- [1] P.Nason, S.Dawson and R.K.Ellis. Nucl.Phys. B303 (1988) 607.
- [2] G.Altarelli et al. Nucl.Phys. B308 (1988) 724.
- [3] P.Nason, S.Dawson and R.K.Ellis. Nucl.Phys. B327 (1989) 49.
- [4] W.Beenakker, H.Kuijf, W.L.Van Neerven and J.Smith. Phys.Rev. D40 (1989) 54.
- [5] W.Beenakker, W.L.Van Neerven, R.Meng, G.A.Schuler and J.Smith. Nucl.Phys. B351 (1991) 507.
- [6] S.Catani, M.Ciafaloni and F.Hautmann. Phys.Lett. B242 (1990) 97; Nucl.Phys. B366 (1991) 135.
- [7] J.C.Collins and R.K.Ellis. Nucl.Phys. B360 (1991) 3.
- [8] G.Marchesini and B.R.Webber. Nucl.Phys. B386 (1992) 215.
- [9] S.Catani and F.Hautmann. Phys.Lett. B315 (1993) 475; Nucl.Phys. B427 (1994) 475.
- [10] S.Camici and M.Ciafaloni. Nucl.Phys. B467 (1996) 25; Phys.Lett. B396 (1997) 406.
- [11] P.Hägler et al. Phys.Rev. D62 (2000) 71502.
- [12] L.V.Gribov, E.M.Levin and M.G.Ryskin. Phys.Rep. 100 (1983) 1.
- [13] E.M.Levin and M.G.Ryskin. Phys.Rep. 189 (1990) 267.
- [14] E.M.Levin, M.G.Ryskin, Yu.M.Shabelski and A.G.Shuvaev. Sov.J.Nucl.Phys. 53 (1991) 657.
- [15] E.M.Levin, M.G.Ryskin, Yu.M.Shabelski and A.G.Shuvaev. Sov.J.Nucl.Phys. 54 (1991) 867.
- [16] M.G.Ryskin, Yu.M.Shabelski and A.G.Shuvaev. Z.Phys. C69 (1996) 269.
- [17] V.A.Saleev and N.P.Zotov. Mod.Phys.Lett. A11 (1996) 25.
- [18] Yu.M.Shabelski and A.G.Shuvaev. Eur.Phys.J. C6 (1999) 313.
- [19] S.P.Baranov and M.Smizanská. Phys.Rev. D62 (2000) 014012.
- [20] S.P.Baranov and N.P.Zotov. hep-ph/0103138.
- [21] M.G.Ryskin, Yu.M.Shabelski and A.G.Shuvaev. Phys.Atom.Nucl. 64 (2001) 120.
- [22] M.G.Ryskin, Yu.M.Shabelski and A.G.Shuvaev. hep-ph/0007238.
- [23] M.G.Ryskin, Yu.M.Shabelski and A.G.Shuvaev. hep-ph/0011111.

- [24] M.Gluck, E.Reya and A.Vogt. Z.Phys. C67 (1995) 433.
- [25] M.Gluck, E.Reya and A.Vogt. Eur.Phys.J C5 (1998) 461.
- [26] G.Marchesini and B.R.Webber. Nucl.Phys. B310 (1988) 461.
- [27] M.A.Kimber, A.D.Martin and M.G.Ryskin. Eur.Phys.J. C12 (2000) 655; hep-ph/9911379.
- [28] M.Ciafaloni. Nucl.Phys. B296 (1988) 49.
- [29] S.Catani, F.Fiorane and M.Ciafaloni. Phys.Lett. B234 (1990) 339; Nucl.Phys. B336 (1990) 18.
- [30] G.Marchesini. In Proc. of the Workshop "QCD at 200 TeV", Erice, Italy (1990), ed. by L.Cifarelli and Yu.L.Dokshitzer, Plenum Press, New-York 1992, p.183.
- [31] S.J.Brodsky, G.P.Lepage and P.B.Mackenzie. Phys.Rev. D28 (1983) 228.
- [32] S.Narison. Phys.Lett. B341 (1994) 73; hep-ph/9503234.
- [33] P.Ball, M.Beneke and V.M.Braun. Phys.Rev. D52 (1995) 3929.
- [34] G.P.Lepage. J.Comp.Phys. 27 (1978) 192.
- [35] D0 Coll., B.Abbott et al. Phys.Lett. B487 (2000) 264.
- [36] D0 Coll., B.Abbott et al. Phys.Rev.Lett. 85 (2000) 5068.
- [37] D0 Coll., B.Abbott et al. Phys.Rev.Lett. 84 (2000) 5478; hep-ph/9907029.
- [38] F.Abe et al. Phys.Rev. D55 (1997) 2546.
- [39] P.Nason et al. "Bottom Production". hep-ph/0003142.
- [40] BEATRICE Coll., M.Adamovich et al. Phys.Lett. B348 (1995) 256.
- [41] BEATRICE Coll., Y.Alexandrov et al. Phys.Lett. B433 (1998) 217.
- [42] ZEUS Coll. M.Derrick et al. Phys.Lett. B349 (1995) 225.
- [43] H1 Coll. Preprint DESY 96-055.
- [44] H1 Coll. Phys.Lett. B467 (1999) 156.
- [45] A.V.Lipatov, V.A.Saleev and N.P.Zotov. Mod.Phys.Lett. A15 (2000) 1727.
- [46] ZEUS Coll. J.Breitweg et al. Eur.Phys.J. C6 (1999) 67.
- [47] A.K.Likhoded and S.R.Slabospitsky. Phys.Atom.Nucl. 60 (1997) 981; 62 (1999) 693; hep-ph/0008230.
- [48] T.Tashiro et al. hep-ph/9810284.

- [49] A.V.Berezhnoy, V.V.Kiselev and A.K.Likhoded. hep-ph/9905555.
- [50] J.Dias de Deus and F.Durães. Eur.Phys.J. C13 (2000) 647.
- [51] Yu.M.Shabelski. hep-ph/0011032.

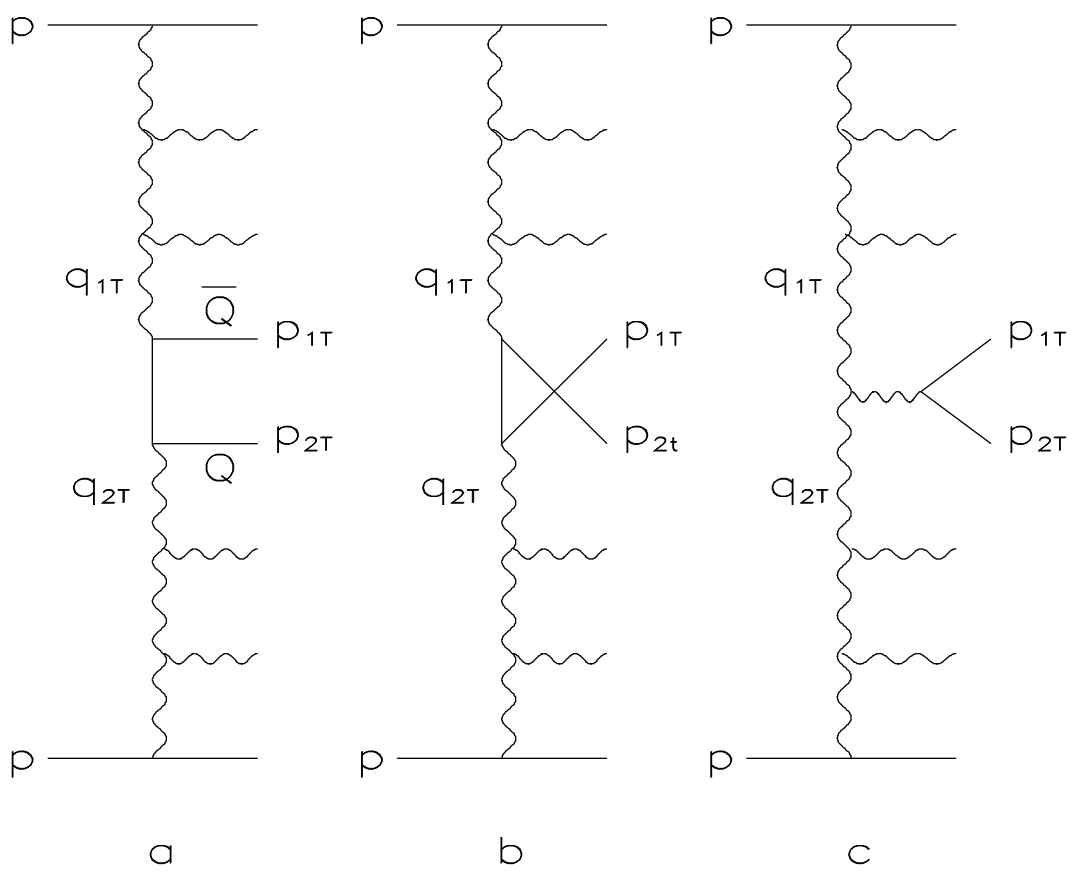


Fig. 1

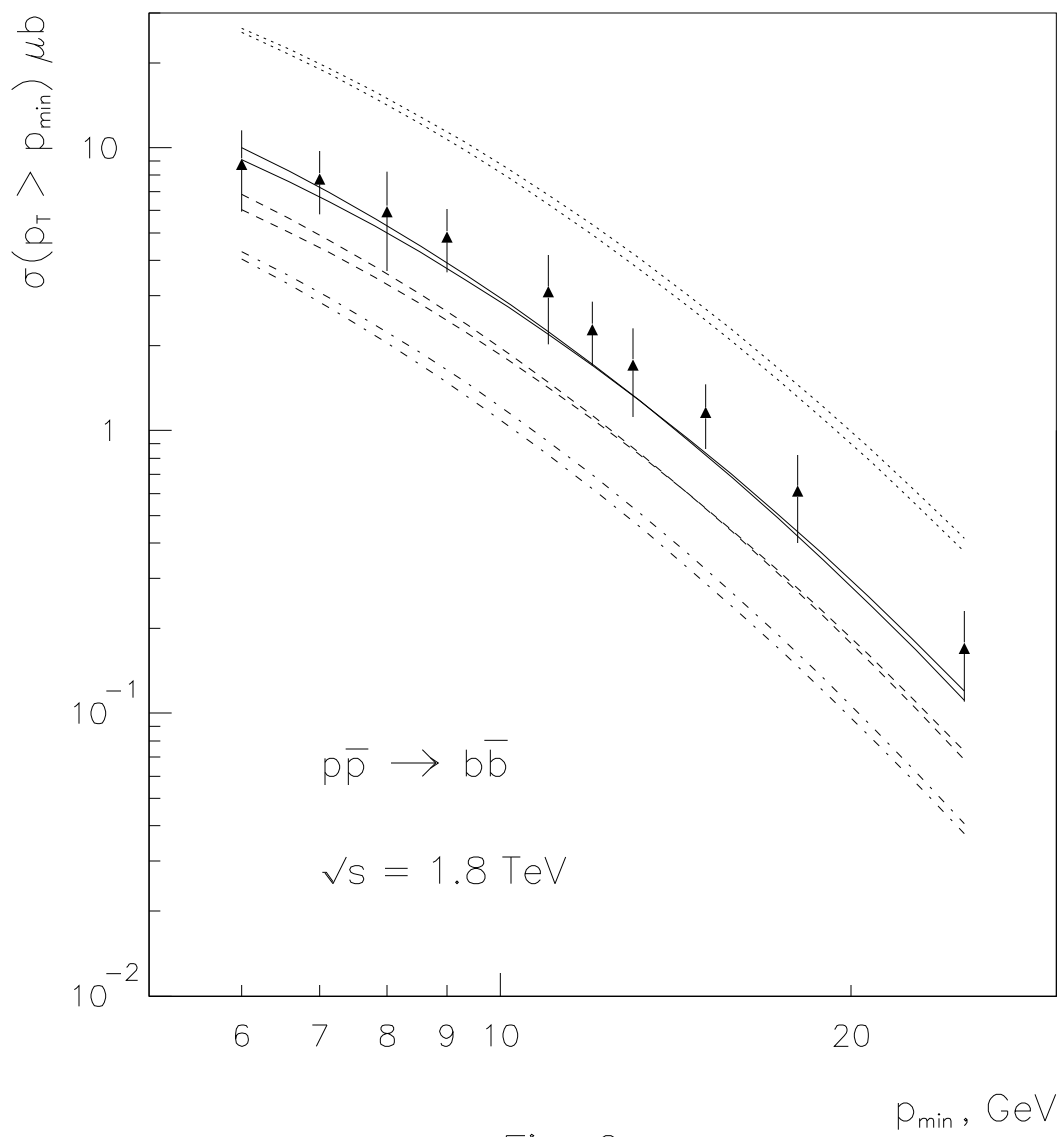


Fig. 2a

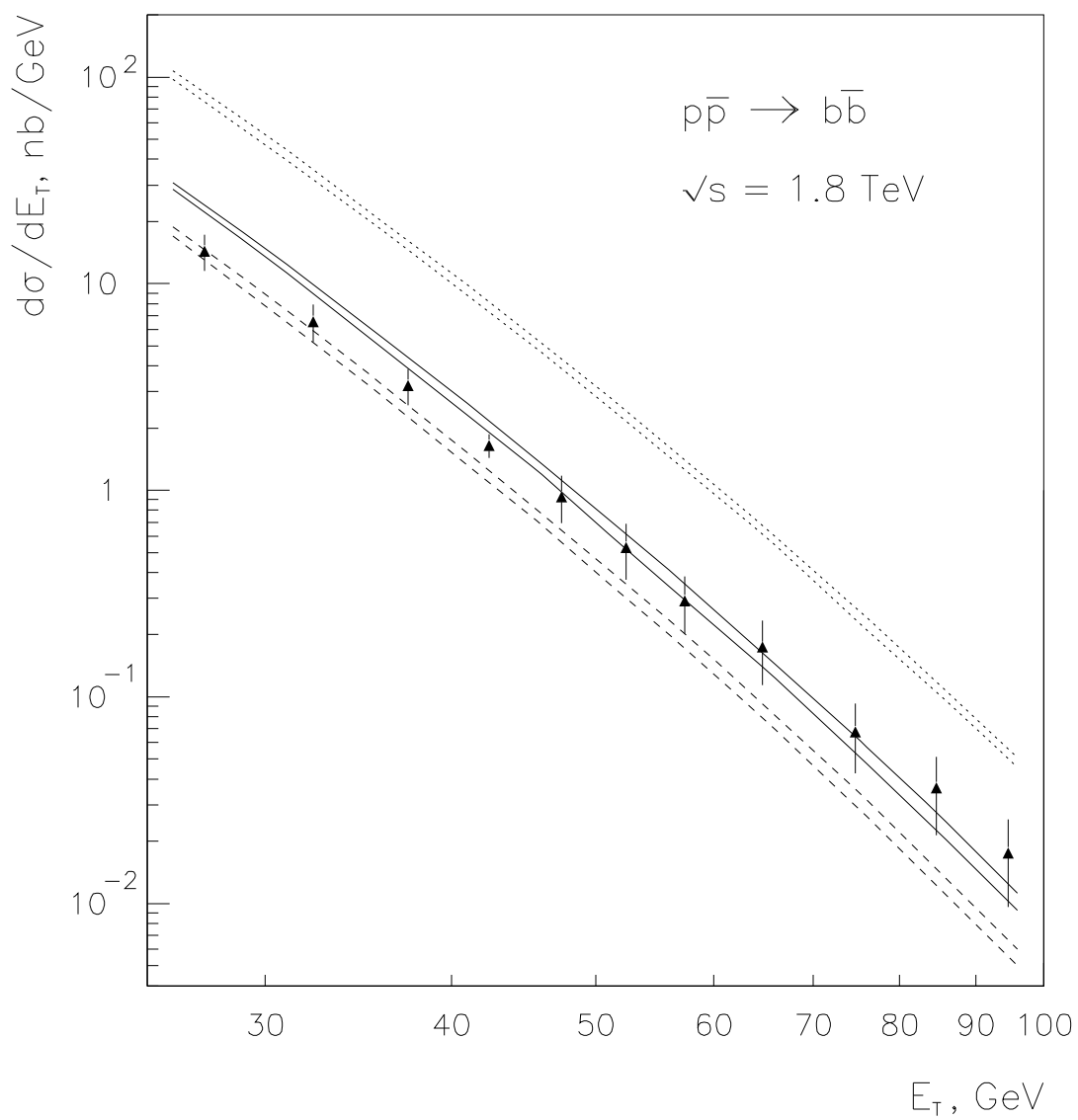


Fig. 2b

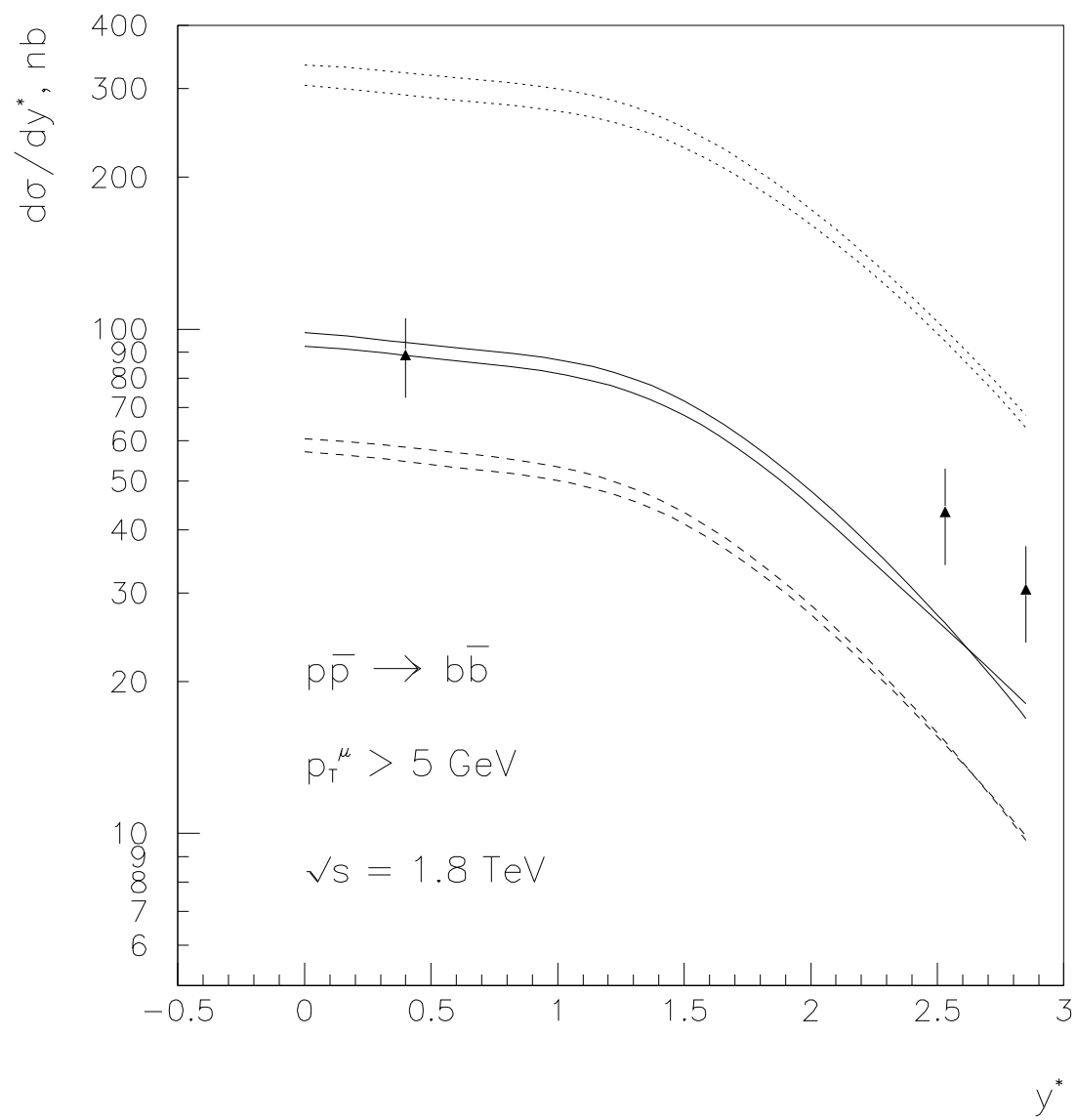


Fig. 3a

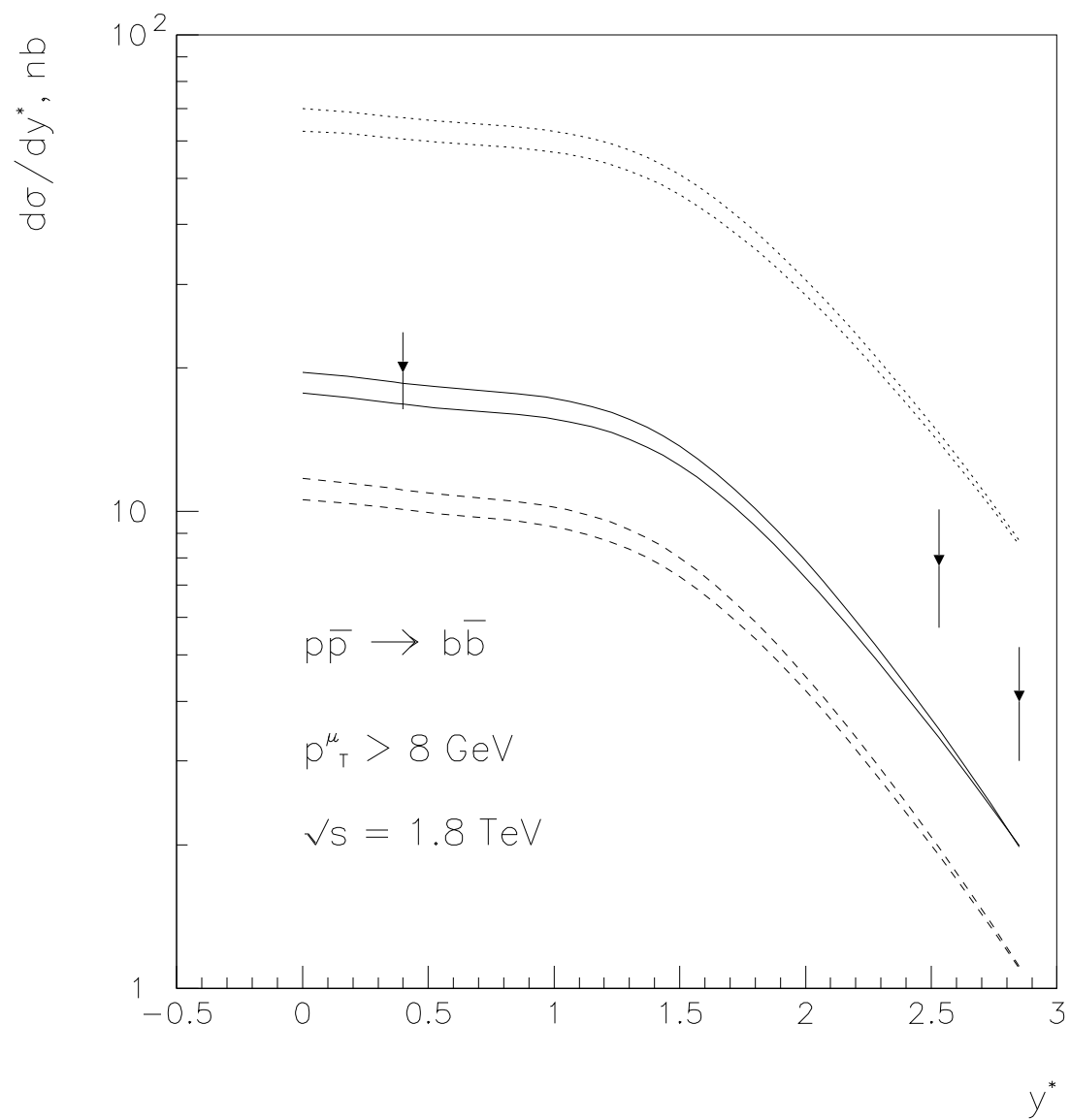


Fig. 3b

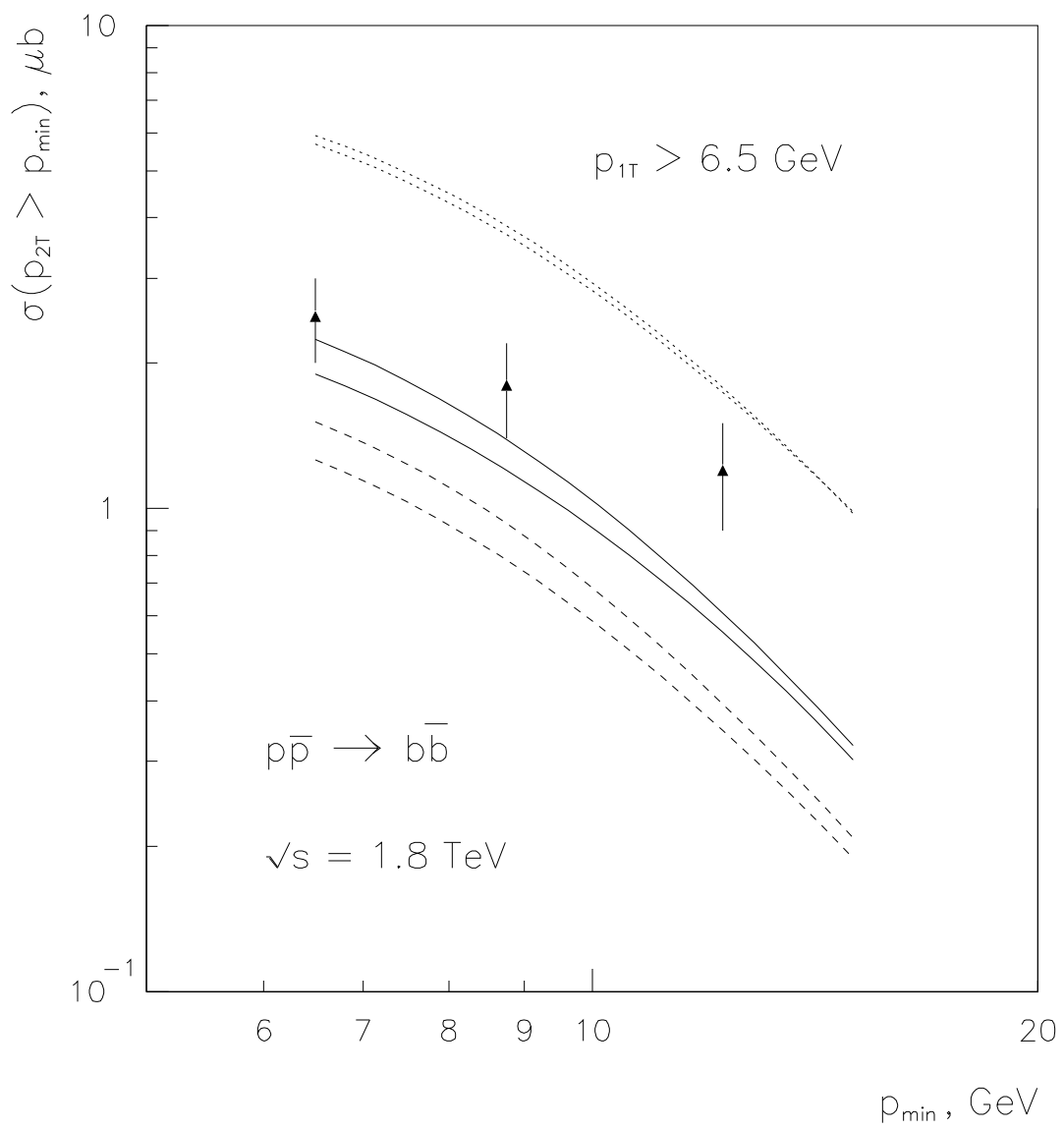


Fig. 4a

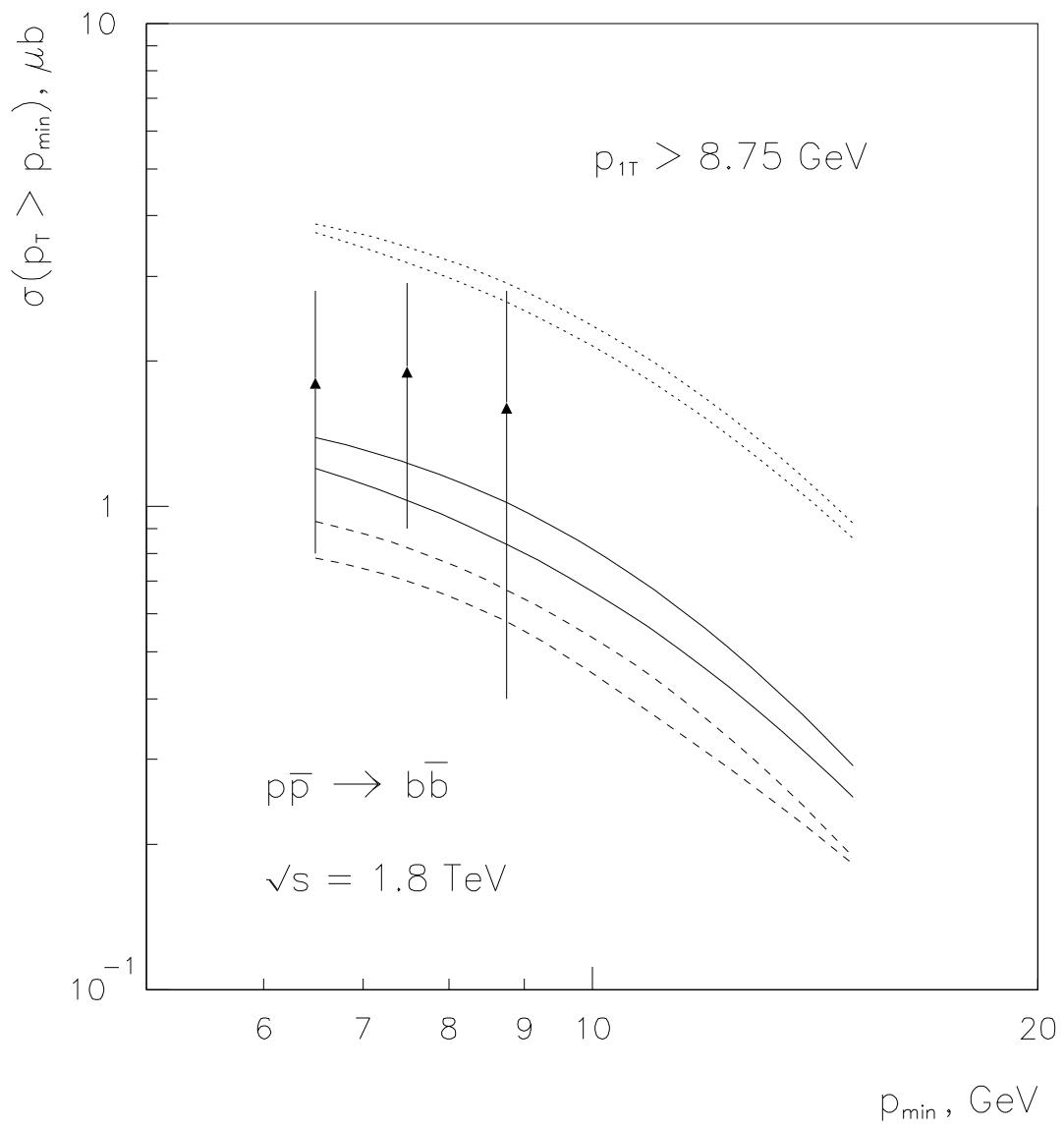


Fig. 4b

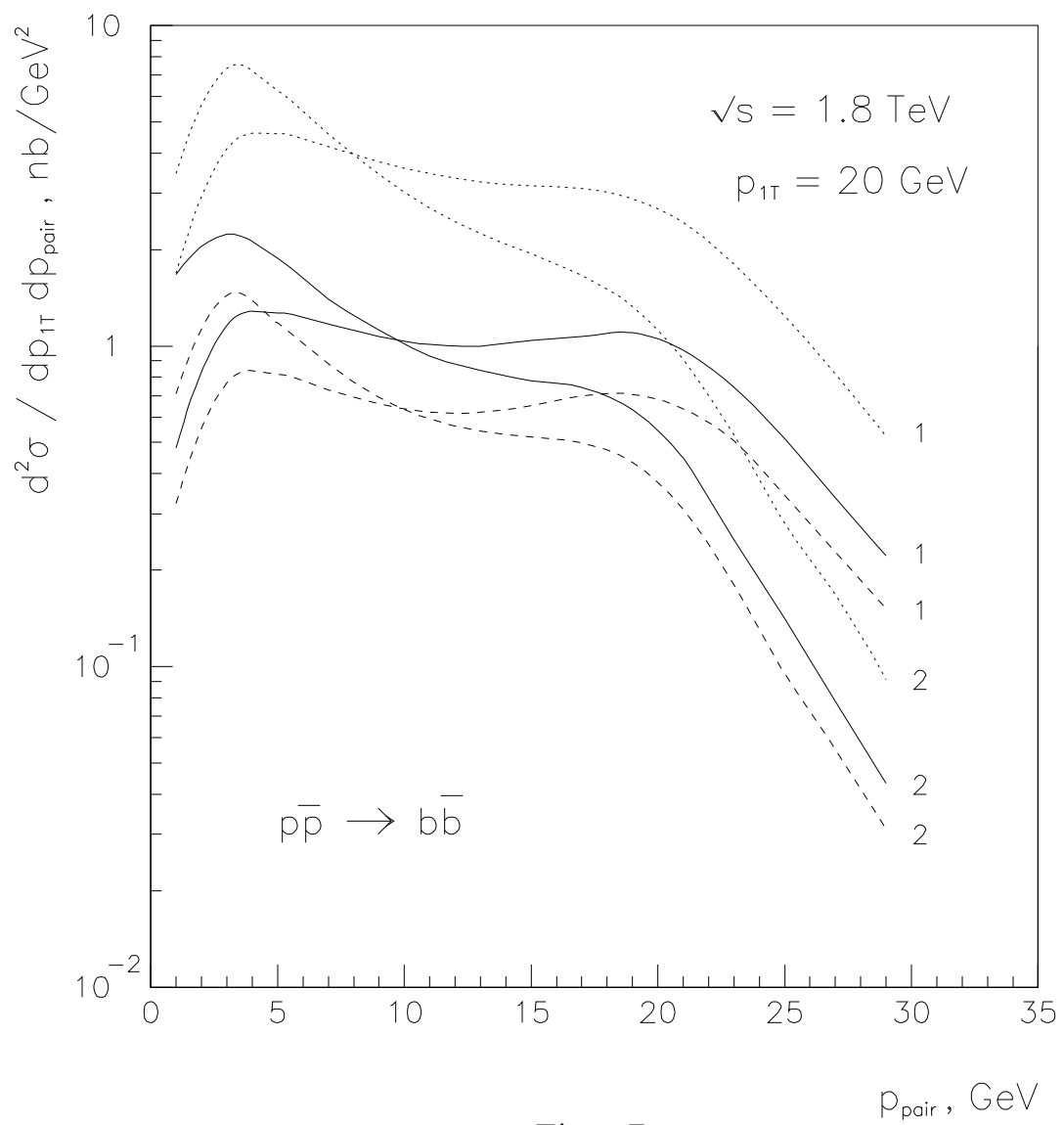


Fig. 5a

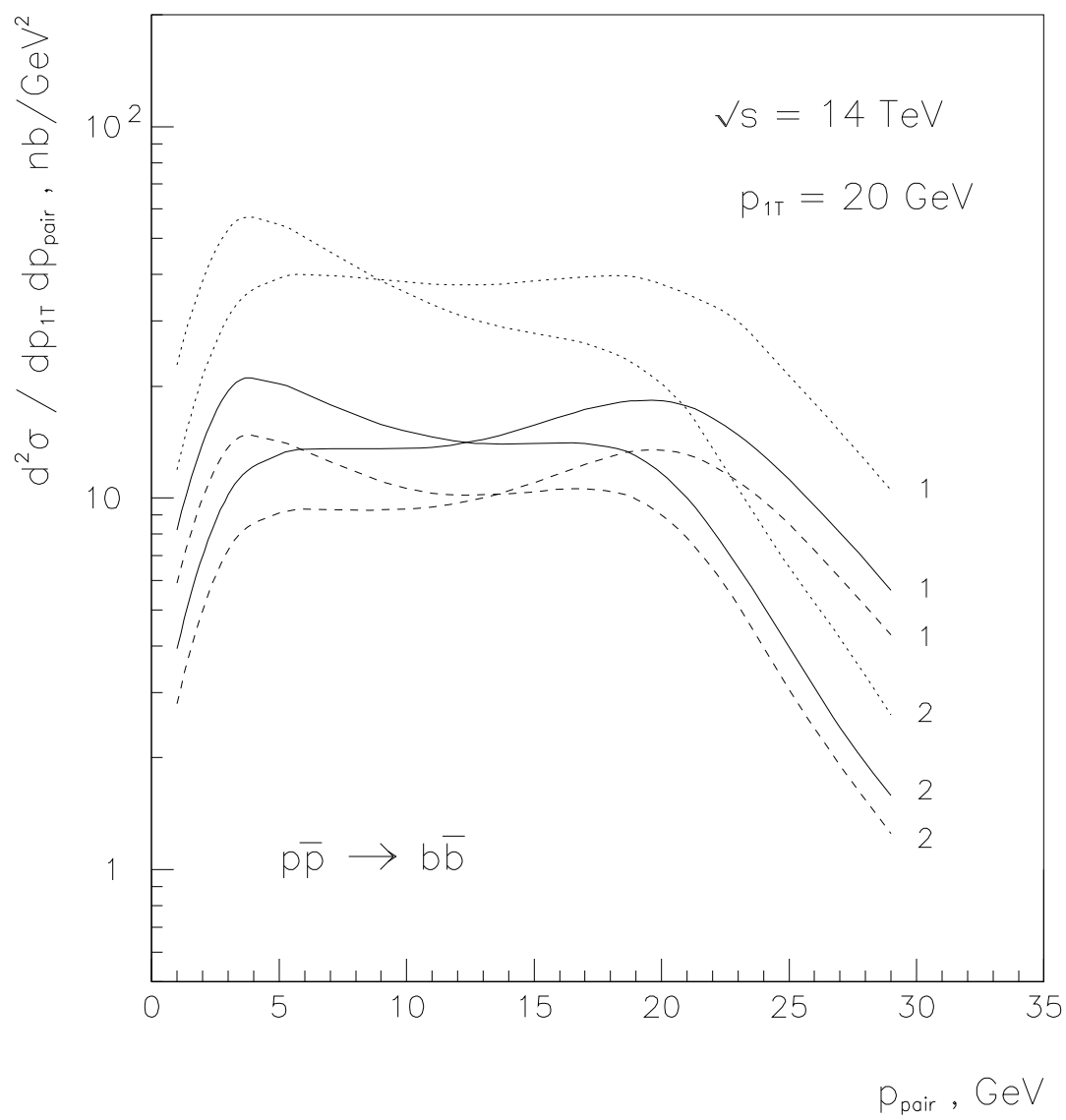


Fig. 5b

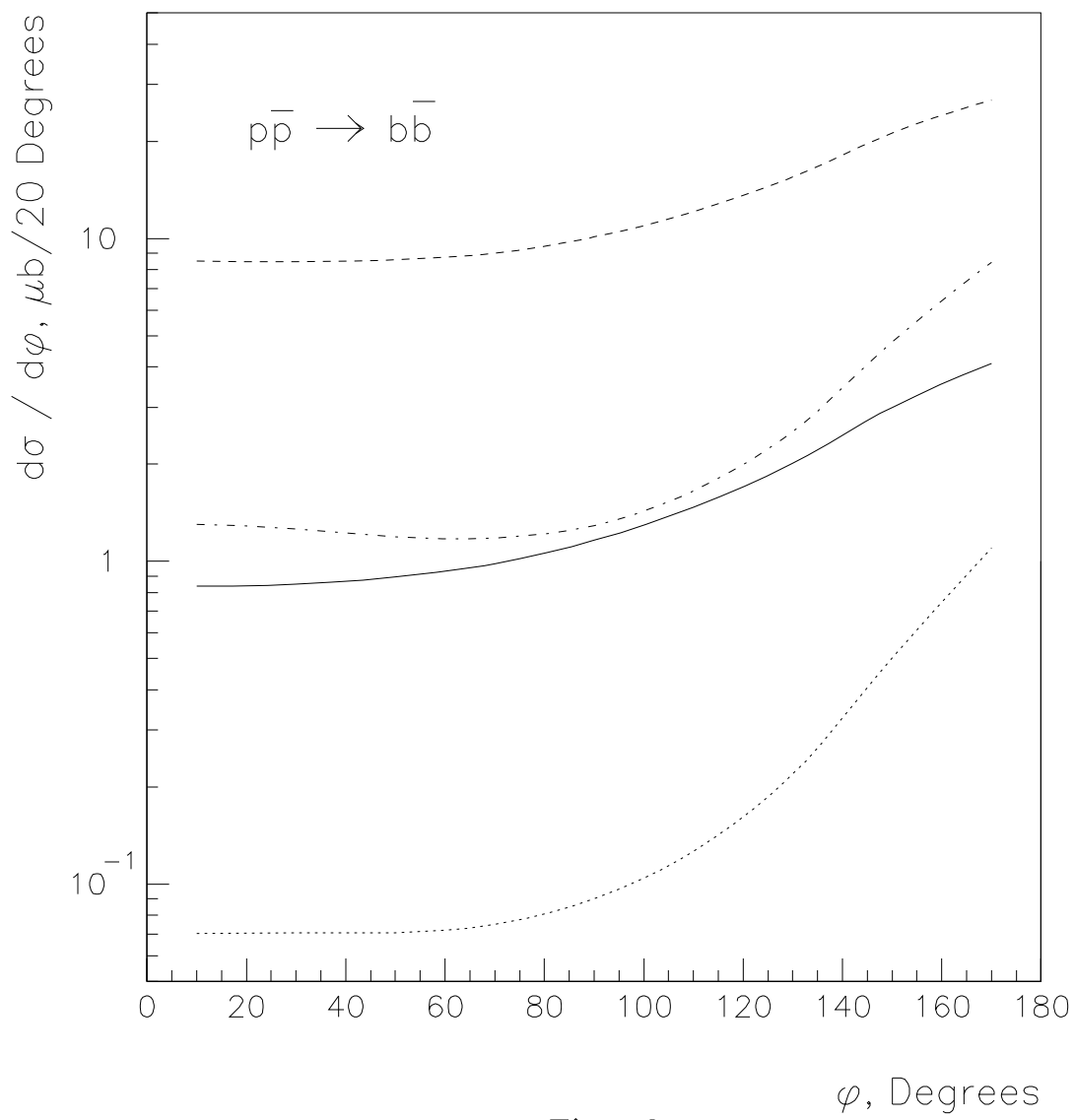


Fig. 6

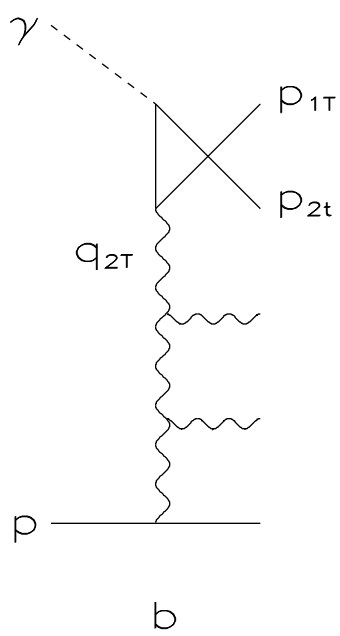
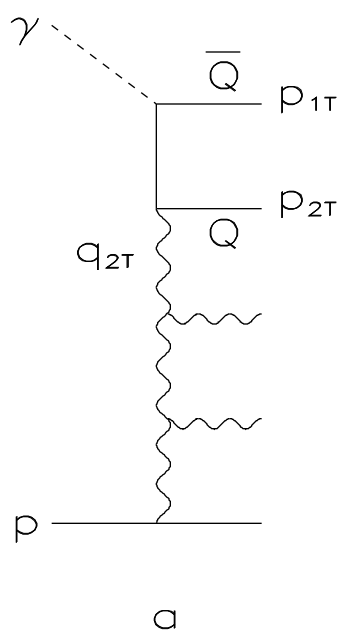


Fig. 7

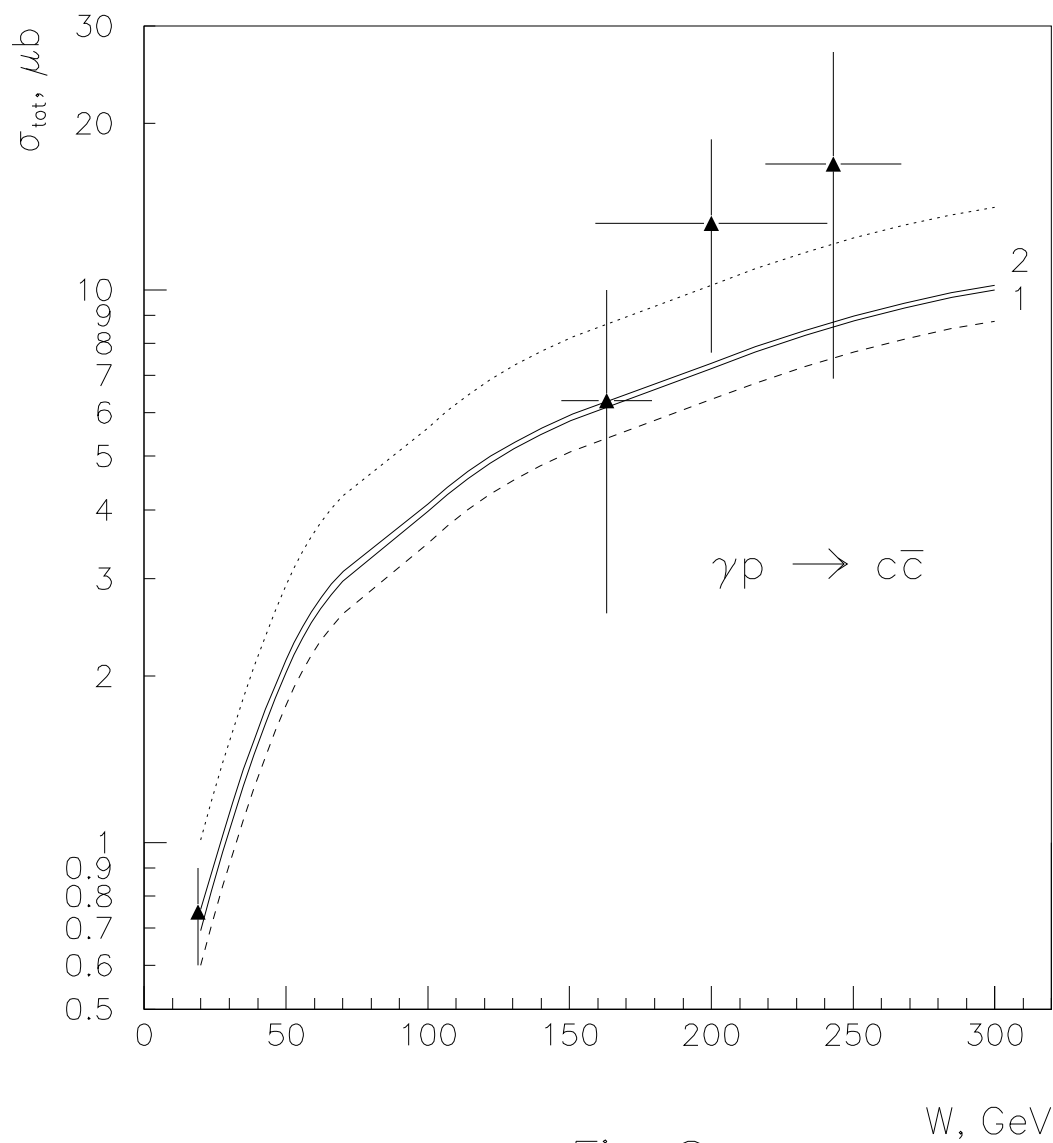


Fig. 8a

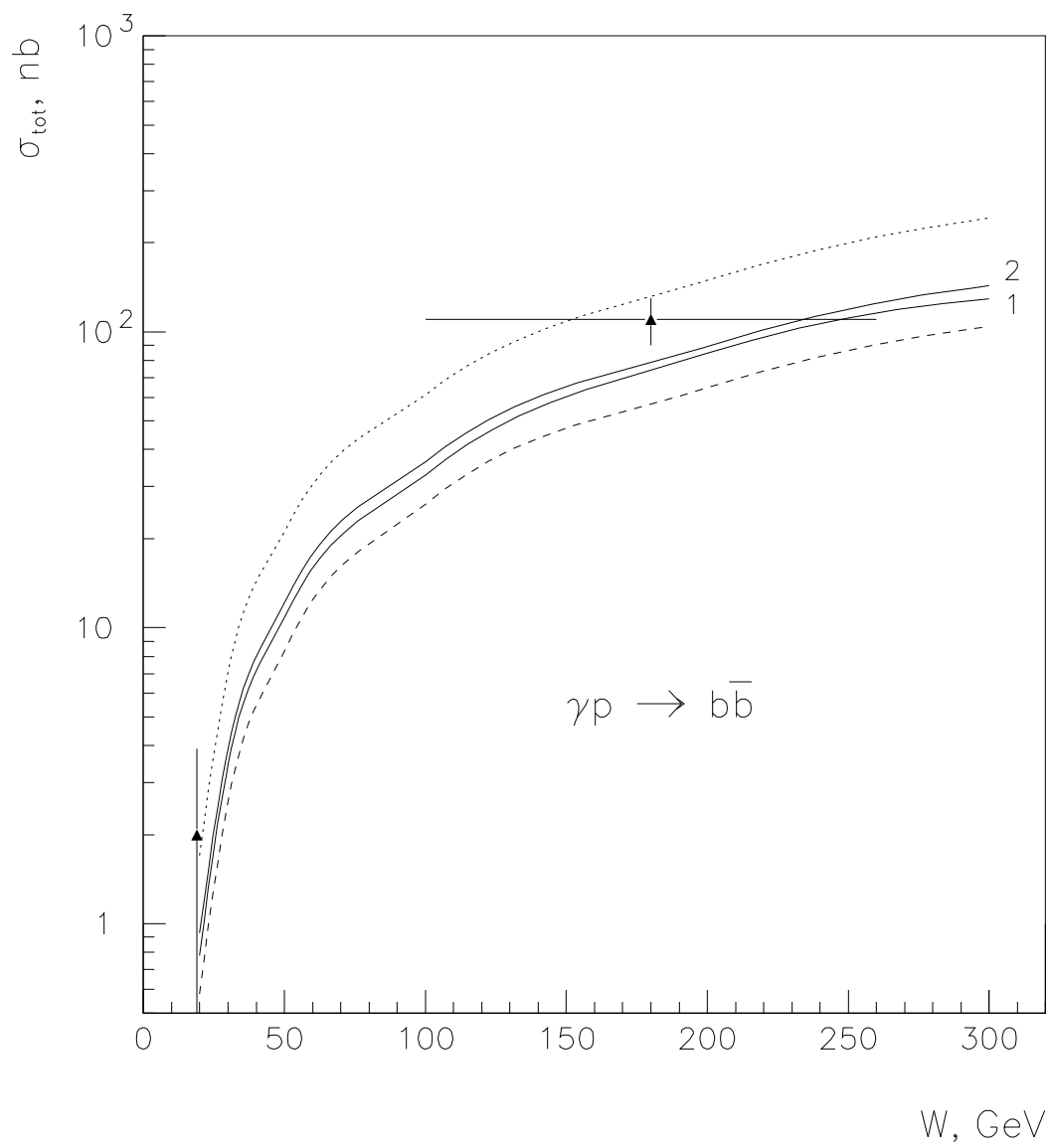


Fig. 8b

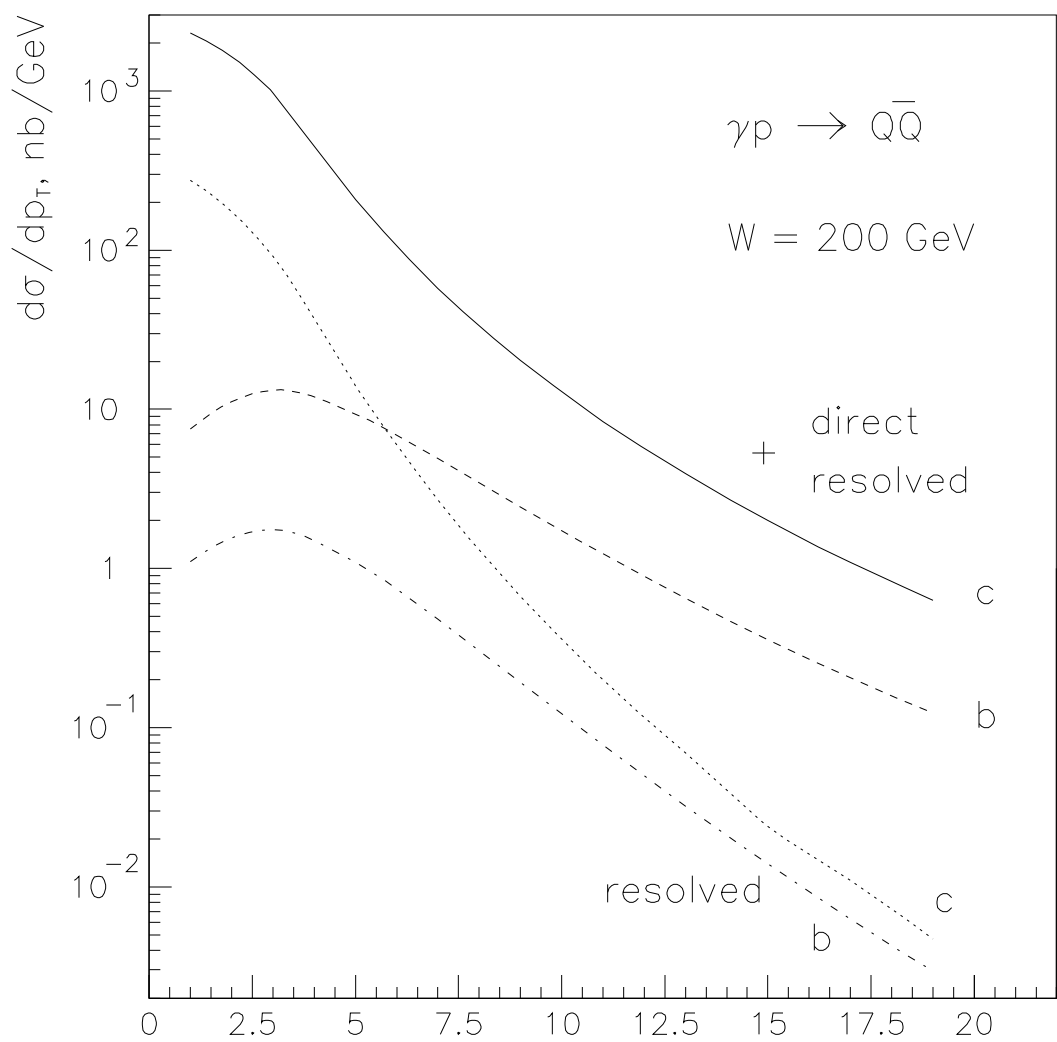


Fig. 9

p_T , GeV

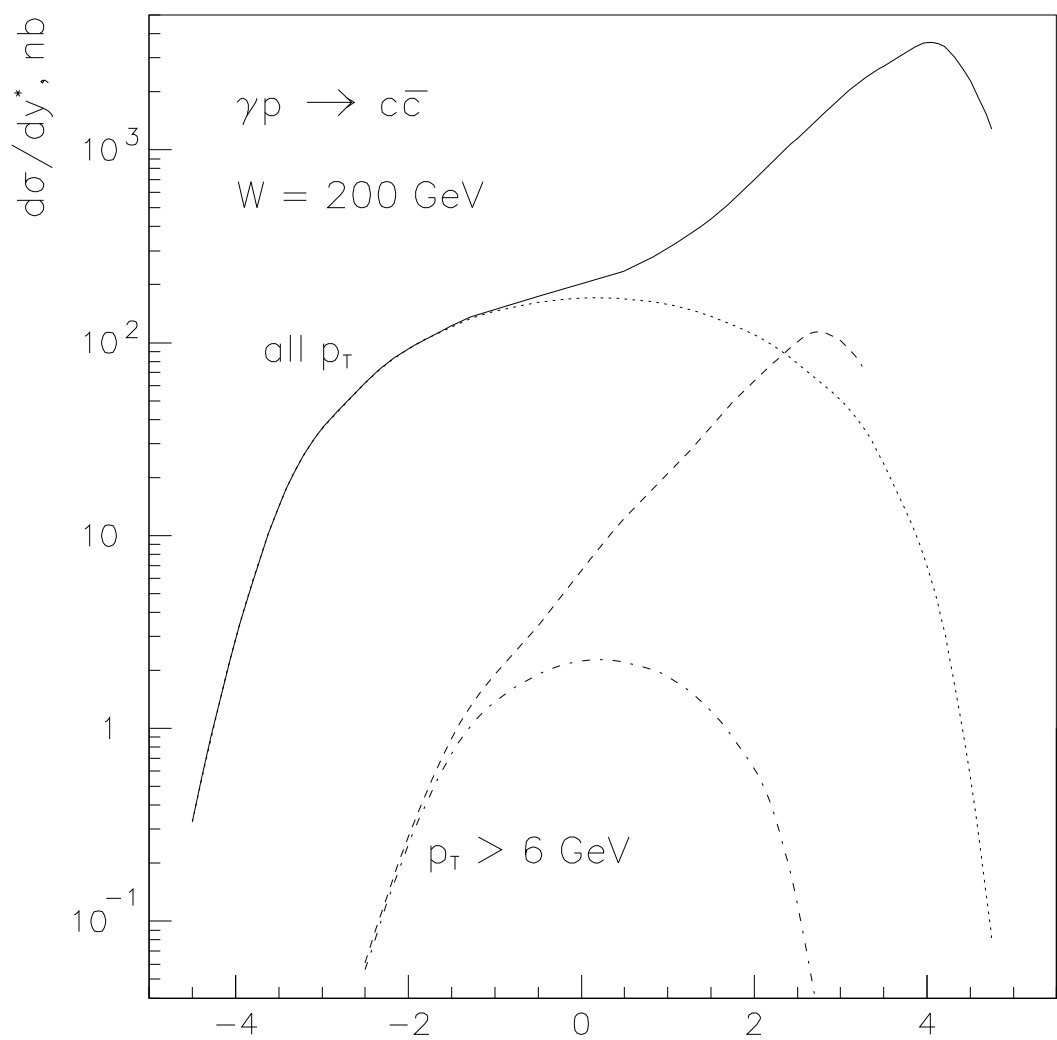


Fig. 10a

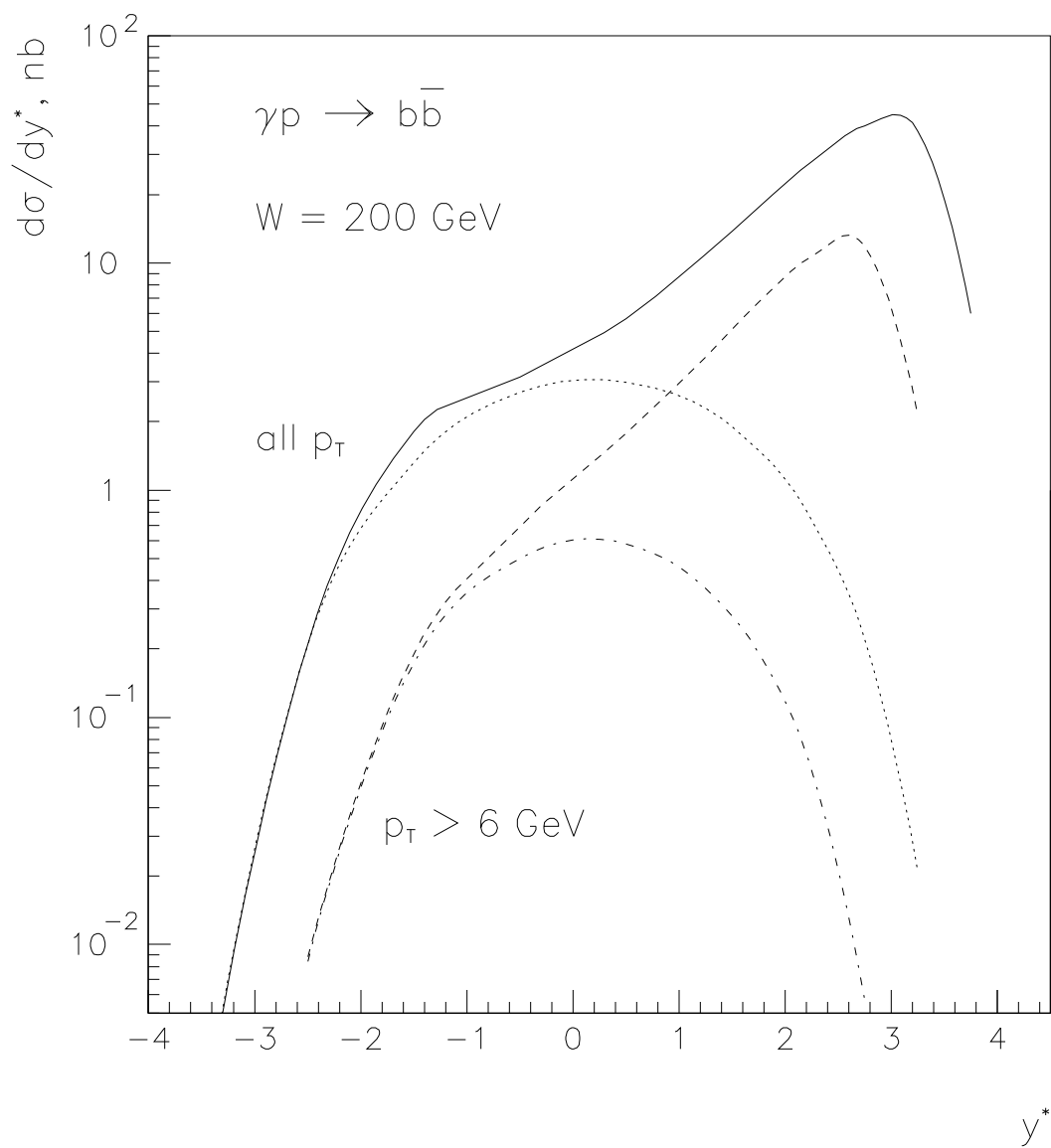


Fig. 10b

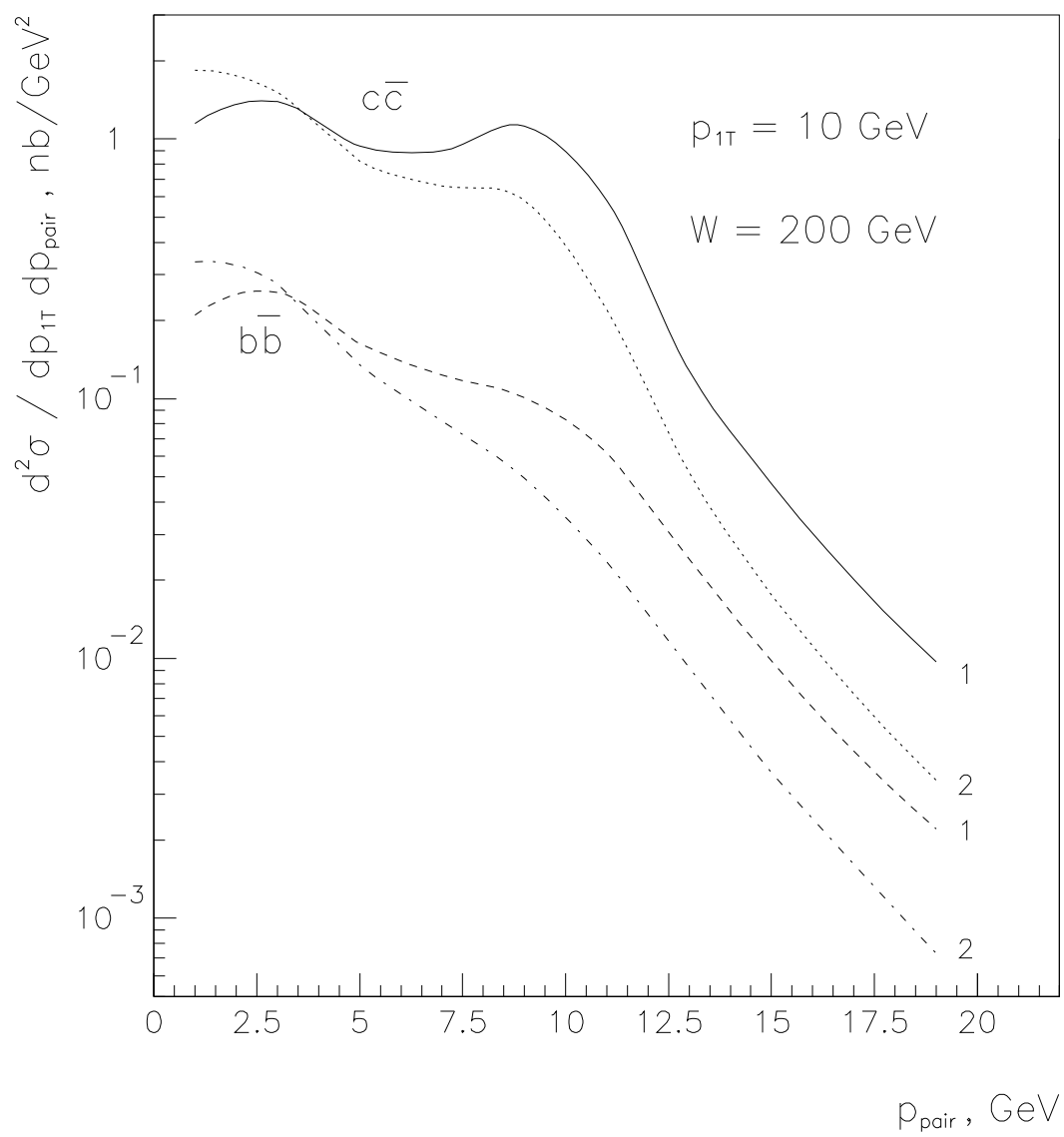


Fig. 11

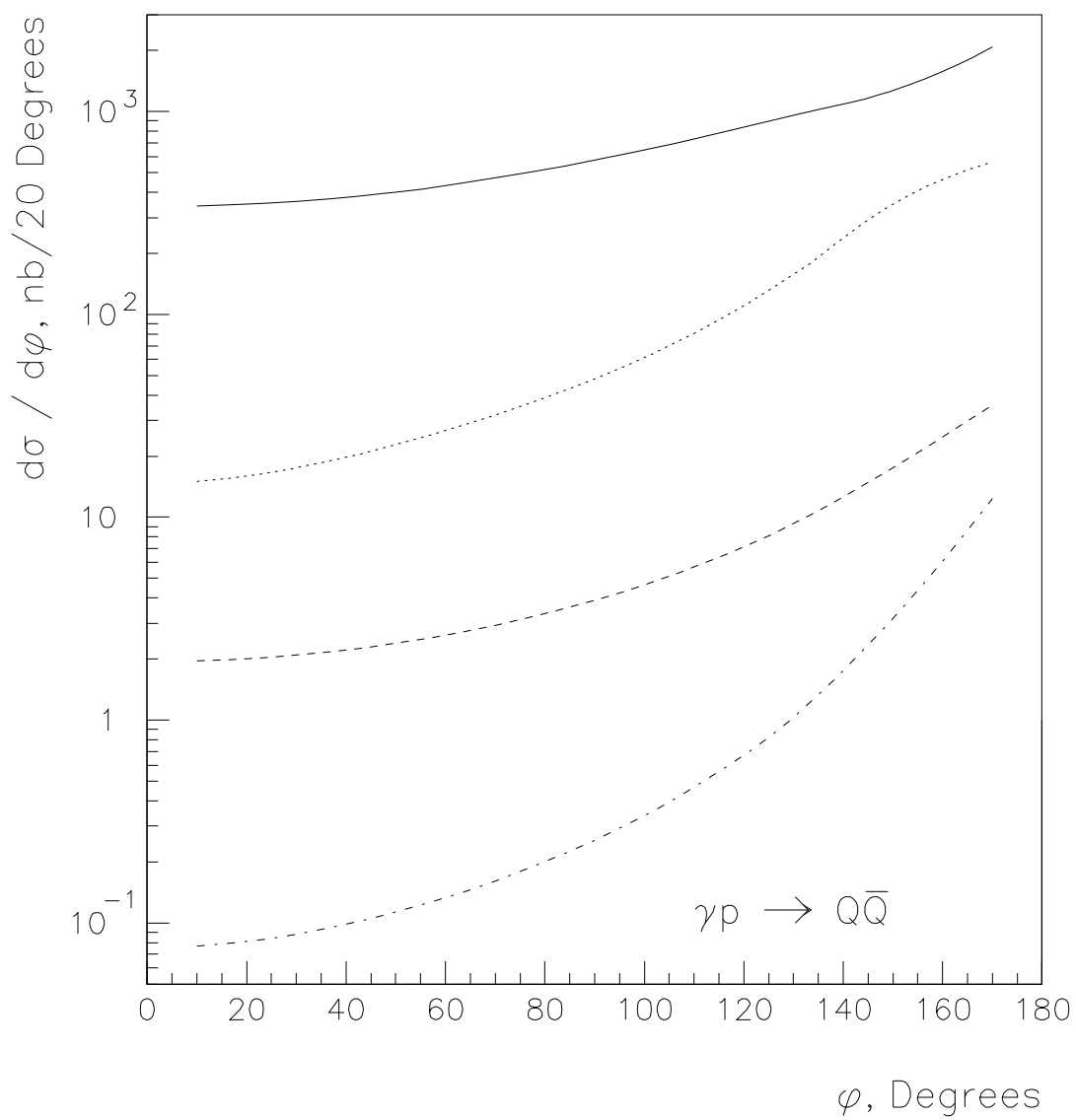


Fig. 12